Dye-Sensitized Solar Cell Photoelectrochemical Tandem System Performance Study: TiO_2 Nanotube/N719, $BiVO_4/TiO_2$ Nanotube, Ti^{3+}/TiO_2 Nanotube for Nitrogen Reduction Reaction to Ammonia

Suharyadi Suharyadi*, Muhammad Iqbal Syauqi, Prita Amelia, Yunita Yunita, and Jarnuzi Gunlazuardi

Department of Chemistry, Faculty of Mathematics and Natural Sciences, Universitas Indonesia, Kampus UI, Depok 16424, Indonesia

* ***Corresponding author:***

tel: +62-85719243866
email: suharyadi@ui.ac.id

Received: July 18, 2022
Accepted: February 17, 2023

DOI: 10.22146/ijc.76270

Abstract: *Ammonia is commonly synthesized through the Haber-Bosch process, which produces large amounts of CO_2 emissions as it is carried out at extreme temperatures and pressures. An alternative technology is needed to synthesize ammonia which consumes less energy and is environmentally friendly. In this research, a Dye-Sensitized Solar Cell Photoelectrochemical tandem system (DSSC-PEC) was developed for the nitrogen reduction reaction (NRR) into ammonia. PEC cells utilized $BiVO_4/TiO_2$ Nanotube ($BiVO_4/TiO_2NT$) as a photoanode for water oxidation. $BiVO_4/TiO_2NT$ was synthesized by the successive ionic layer adsorption and reaction (SILAR) with the cycles variation of 10, 15, and 20 cycles. The optimization method for 20 cycles (20s) gave the highest photocurrent of 0.352 mA/cm^2. As a cathode where the nitrogen reduction reaction to ammonia takes place, Ti^{3+}/TiO_2NT was used. DSSC based on TiO_2NT/N719 with an efficiency of 1.13% was used as an energy booster in the reaction. Using this system with an electrodes area of 3 cm^2, under visible light irradiation on photoanode and DSSC while dark at the cathode, the rate of ammonia production, analyzed using the phenate method, was 0.022 μmol.h^{-1}.cm^{-2} with solar to chemical conversion (SCC) efficiency of 0.003%.*

Keywords: *$BiVO_4/TiO_2NT$; DSSC-PEC; SILAR; NRR; ammonia*

■ INTRODUCTION

Ammonia (NH_3) is an important chemical and is widely used in various chemical industrial applications and processes, especially in making fertilizers as a nutrient for plants [1]. Ammonia is produced through the Haber-Bosch process using H_2 and N_2 at high pressure (> 200 bar) and high temperature (> 673 K) [2]. However, the use of natural gas as a source of H_2 obtained by steam reforming of hydrocarbon sources consumes about 1–2% of the world's energy annually by releasing hundreds of millions of tons of CO_2 annually [3]. To minimize the negative environmental impact, it is necessary to find alternative technologies for making ammonia with low energy requirements, abundant raw materials, and not producing CO_2 gas. One way that has attracted the attention of many parties is to carry out nitrogen reduction reactions (NRR) through photoelectrochemistry [4].

Photoelectrochemistry (PEC) is a combination of photochemical and electrochemical processes. In the PEC setting, NRR occurs at the cathode site using a catalyst having an active site capable of activating the stable triple bond of N_2, while at the anode, a catalyst that can oxidize water well under visible light exposure is desired. Several studies have been conducted using the PEC method, Liu et al. [5] used a photoelectrochemical method for the reduction of N_2 to ammonia using black phosphorus-produced ammonia with a Faraday efficiency of 23.3%. Liu et al. [6] have developed a photocatalytic method using TiO_2 nanoparticles with oxygen vacancy for nitrogen fixation with the highest ammonia generation rate of 116 μmol.g^{-1}.h^{-1}.

TiO_2 is one of the semiconductors that is widely used as a photoelectrode in PEC cells with various advantages such as high efficiency, low cost, physical and

chemical stability, wide availability, non-corrosive, and environmentally friendly [7]. TiO_2 in the form of 1D nanostructures such as nanotubes (TiO_2NT) exhibits a very large surface-to-volume ratio and significantly increased light absorption [8-9]. It is well known that the population of Ti^{3+} in TiO_2 could serve as an active site to carry out the NRR reaction [2]. However, to be used as a photoanode, TiO_2 is still lacking. As it has a band gap of about 3.2 eV, the absorption only occurs in the UV region; TiO_2 is not an efficient photocatalyst under sunlight irradiation, which contains > 95% infrared and visible light while only ~5% UV light. Therefore, it is very important to develop photocatalysts that can be used in both UV light (290–400 nm) and visible light (400–700 nm) to increase the efficiency of photocatalysis [10].

It is necessary to modify TiO_2, one of which is the $BiVO_4$/TiO_2NT heterojunction, to increase light absorption in the visible light region. $BiVO_4$ has a band gap of 2.4 eV. Zhu et al. [11] reported that the $BiVO_4$/TiO_2 heterojunction has 1.4 times higher photocatalytic activity compared to pure $BiVO_4$. The incorporation of TiO_2 with another semiconductor not only affects the light absorption ability but can increase the specific surface area and pore diameter.

The use of the Dye-Sensitized Solar Cell Photoelectrochemical (DSSC-PEC) tandem system can increase light absorption in the visible light region compared to without DSSC. Several studies have been conducted on DSSC-PEC tandem cells, among others; Surahman [12] conducted the development of PEC cells using CdS nanoparticle sensitized TiO_2 nanotube arrays for hydrogen production with hydrogen gas formation rate of 13.44 L/min and energy efficiency cells through the process of breaking water by 4.78%. Samsudin et al. [13] developed a tandem DSSC-PEC system with thin films of $BiVO_4$/TiO_2NT for hydrogen production to produce 692 mol of hydrogen in 120 min.

Research developments related to the performance of Ti^{3+}/TiO_2NT for NRR applications, $BiVO_4$/TiO_2NT as a photoanode, and DSSC N719 have been widely reported. However, the combined system of PEC-based $BiVO_4$/TiO_2NT as photoanode, Ti^{3+}/TiO_2NT as cathode, and DSSC-based N719 as a whole tandem system to do NRR to ammonia, as far as the authors' knowledge, has not been reported. In this study, an evaluation of the performance of the DSSC-PEC tandem system for the NRR to ammonia was carried out using Ti^{3+}/TiO_2NT as a cathode. As a photoanode, TiO_2NT-modified $BiVO_4$ was used using the SILAR method. As for the DSSC zone, TiO_2NT/N719 sandwich cells, I^-/I_3^-, and Pt/FTO electrolytes are used. This research is expected to contribute to the development of alternative methods for producing environmentally friendly ammonia with relatively low energy consumption.

■ EXPERIMENTAL SECTION

Materials

The materials used in this study were titanium plate (99.6% purity Baoji Jinsheng Metal Material Co. Ltd), acetone (C_3H_6O) (≥ 99.5% purity Sigma-Aldrich), bismuth nitrate pentahydrate ($Bi(NO_3)_3.5H_2O$) (98% purity Sigma-Aldrich), ethanol (C_2H_5OH) (99.9% purity Sigma-Aldrich), ethylene glycol (C_2H_6O) (99.8% purity Sigma-Aldrich), ammonium vanadate (NH_4VO_3) (≥ 99.0% purity Sigma-Aldrich), FTO, sodium sulfate (Na_2SO_4) (≥ 99% purity Sigma-Aldrich), trisodium citrate ($Na_3C_6H_5O_7$) (≥ 98% purity Sigma-Aldrich), sodium hypochlorite (NaOCl) from Sigma-Aldrich, nitric acid (HNO_3) (65% purity Sigma-Aldrich), sodium hydroxide (NaOH) (≥ 98% purity Sigma-Aldrich), ammonium chloride (NH_4Cl) (≥ 99.5% purity Sigma-Aldrich), sodium nitroprusside (SNP) from Sigma-Aldrich, dye N719 (95% purity Sigma-Aldrich), Nafion membrane 117, and phenol (99% purity Sigma-Aldrich), and deionized water from OneMed.

Instrumentation

TiO_2NT and $BiVO_4$/TiO_2NT were characterized using XRD (X'pert PRO merk PANalitycal MPD PAW3040/60), FTIR (Shimadzu IR Prestige 21), UV-Vis DRS (Shimadzu UV-2450), SEM-EDX (Quanta 650 of Thermo Scientific), and Potentiostat (PAR-VersaStat II). While Ti^{3+}/TiO_2NT was characterized using FTIR, UV Vis DRS, and Potentiostat.

Procedure

Synthesis of TiO_2 nanotubes (TiO_2NT) and Ti^{3+}/TiO_2NT

The titanium plate (0.3 mm thickness, 99.6%) was sanded with 1000 and 1500 cc abrasive paper, then sonicated in a solution of acetone, ethanol, and air deionized for 16 min, then dried in air. Anodization was conducted in an electrochemical cell consisting of two electrodes, a Ti plate (4 cm × 1.5 cm × 0.02 cm) as an anode, and stainless steel as a cathode. Ethylene glycol solution containing 0.3% NH_4F and 2% H_2O was used as an electrolyte. The distance between the two electrodes is set to about 1.5 cm. The anodizing potential was carried out at 40 V, and the anodization time of 45 min. After the anodization process, the samples were rinsed with deionized water and dried in the air, then calcined at a temperature of 450 °C for 2 h with a temperature rise rate of 10 °C/min^{-1} [12].

The synthesis of Ti^{3+}/TiO_2NT used an electrochemical reduction method with a three-electrode system with TiO_2NT as the working electrode, Pt as the counter electrode, and Ag/AgCl as the reference electrode. Then put into 0.1 M Na_2SO_4 electrolyte solution and given a potential of -1.5 V for 20 min [14].

Synthesis of $BiVO_4/TiO_2$NT

A solution of 50 mL $Bi(NO_3)_3$ 0.02 M was prepared in beaker 1, and 50 mL NH_4VO_3 0.02 M was prepared in beaker 2. The solvent for NH_4VO_3 is deionized water, while the solvent for $Bi(NO_3)_3$ is a mixture of nitric acid and water ($V_{nitric\ acid}$:V_{water} = 1:19). TiO_2 nanotube plate substrate was immersed in beaker 1 for 30 s and then immersed in beaker 2 for 30 s. This process is defined as one cycle. The process was done for 10, 15, and 20 cycles in ultrasonication, denoted as 10 s, 15 s, and 20 s, respectively. Each immersion of the TiO_2 nanotube plate was rinsed with deionized water and dried in the air after all cycles were completed. Then, the prepared samples were calcined at 500 °C for 2 h at a heating rate of 10 °C.min^{-1} [15].

DSSC fabrication, TiO_2NT/N719

TiO_2 nanotubes were immersed in a 300 µM N719 color solution (ethanol solvent) for 24 h. After 24 h of immersion, TiO_2NT/N719 was cleaned with ethanol and dried in the air [16]. TiO_2NT/N719 as an anode, electrolyte I^-/I_3^-, and Pt/FTO as a cathode. The arrangement of the DSSC cells follows a sandwich cell configuration, electrolyte I^-/I_3^- is dripped on the surface of the anode (TiO_2NT/N719), then parafilm as a separator between the anode and cathode to avoid short circuit current, and then closed with a cathode (Pt/FTO).

DSSC-PEC preparation and performance evaluation

PEC cells consist of $BiVO_4/TiO_2$NT as a photoanode and Ti^{3+}/TiO_2NT as a dark cathode. TiO_2NT/N719 as an anode in the DSSC zone is connected

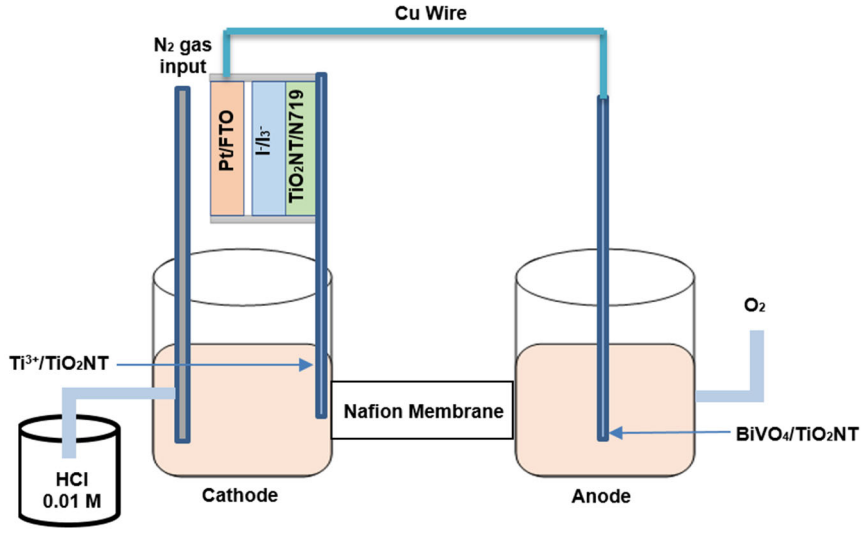

Fig 1. Schematic of DSSC-PEC Tandem System for A and B conditions (A: dark cathode, B: full irradiation)

to the PEC cathode (Ti^{3+}/TiO_2NT), while the PEC photoanode ($BiVO_4/TiO_2NT$) is connected to the DSSC cathode (Pt/FTO) with a copper wire. The evaluation of the system to produce NH_3 was conducted with two irradiation conditions. The A condition (dark cathode) was when the DSSC and anode were illuminated while the cathode was dark. The condition when all the systems (DSSC and PEC) were illuminated is denoted with B condition (full irradiation). The efficiency of ammonia conversion was calculated using the Solar to Chemical Conversion (SCC) equation as shown in Eq. (1) [2]:

$$\text{SCC Efficiency (\%)} = \frac{\Delta G \text{ for } NH_3 \text{ (J/mol)} \times NH_3 \text{ formed (mol)}}{\text{total input energy (W)} \times \text{reaction time (s)}} \times 100\% \quad (1)$$

■ RESULTS AND DISCUSSION

Characterization of Photoanode Materials

Fig. 2(a) shows the FTIR spectra of the synthesized materials. The results of FTIR characterization on TiO_2NT and $BiVO_4/TiO_2NT$ contained OH groups stretching at wavenumbers 3400–3000 cm^{-1}, OH bending at wavenumbers 1800–1400 cm^{-1}, Ti-O-Ti at wavenumbers 900–700 cm^{-1}. The wide peak at a wave number of around 400–700 cm^{-1} is the asymmetric stretching of the vanadate due to the $BiVO_4$ monoclinic.

Fig. 2(b) shows the results of the XRD characterization of TiO_2NT and $BiVO_4/TiO_2NT$. In the TiO_2NT diffraction pattern, diffraction peaks were observed at positions 2θ: 25.31°, 35.05° 38.26°, 40.11°, 48.09°, 53.05°, 53.88°, 55.06°, 63.06°, 70.60°, 76.19°, and 82.34°. Based on JCPDS data No. 00-02101272, the typical peaks of anatase crystals are at the 2θ positions: 25.281°, 37.801°, 38.576°, 48.050°, 53.801°, 55.062°, 70.311°, 75.032°, 76.020°, and 93.221°. Meanwhile, based on data from JCPDS No. 00-044-1294, the typical peaks of titanium metal are in the 2θ positions: 35.09°, 38.43°, 40.17°, 53.01°, 62.94°, 70.66°, 76.23°, 77.38°, and 82.30°. Based on the JCPDS data, it is known that the crystalline phase formed in the synthesized TiO_2NT is the anatase phase. In the $BiVO_4/TiO_2NT$ diffraction pattern, additional diffraction peaks were observed, which were then compared with JCPDS data No. 14-0688 for the monoclinic scheelite phase $BiVO_4$ [17]. It can be observed at 10 cycles of SILAR deposition, and there was 1 additional peak at position 2θ 18.88° (110); at 15 cycles, there was 1 additional peak at position 2θ 28.91° (121), and at 20 cycles, there were 3 additional peaks at positions 2θ 18.88° (110), 28.91° (121), and 30.59° (040) indicating the presence of $BiVO_4$. The intensity of the XRD peak should increase along with the increase of $BiVO_4$ thickness. However, our work observed an anomaly of difference peak observed at 10 and 15 cycles. This phenomenon may be caused by several factors: 1) The amount of $BiVO_4$ concentration on TiO_2NT was too small and not well dispersed for 10 and 15 cycles; 2) Different properties on the TiO_2NT substrate; 3) Physical damage of the sample, or; 4) The unstandardized SILAR deposition process, as the difference in each dipping time, pH solution, might lead to a different crystal growth orientation [18]. Of course, to prove these hypotheses, more elaborate work should be done. However, for this work, the samples were used as it is. Thus, based on the result of the three cycles, the best is SILAR with 20 cycles with 3 peaks of $BiVO_4$; this is because more $BiVO_4$ has been deposited on the TiO_2NT surface so that the dominant $BiVO_4$ facet is formed.

Fig. 2(c) shows UV-DRS spectra to determine the band gap value of the synthesized materials. Bandgap values can be calculated using the Tauc plot of the Kubelka-Munk function:

$$F(R)h\nu^2 = B(h\nu - Eg) \quad (2)$$

The equation is a direct band gap. Based on this equation, the bandgap value of TiO_2NT is 3.21 eV. Based on the literature, the band gap value of TiO_2NT is 3.20 eV [19]. This band gap value indicates that the synthesized TiO_2NT was in the anatase phase. Furthermore, the synthesized TiO_2NT was deposited with $BiVO_4$ through the SILAR process with 3 cycle variations, namely 10, 15, and 20 cycles. The resulting band gap value decreases as the number of cycles increases, where the band gap value is 2.83 eV, 2.81 eV, and 2.79 eV, respectively. Based on the literature, the band gap value of $BiVO_4$ is 2.4 eV [20], the bandgap value which is between the bandgap value of pure TiO_2NT anatase (3.20 eV) and $BiVO_4$ monoclinic (2.40 eV) indicates the

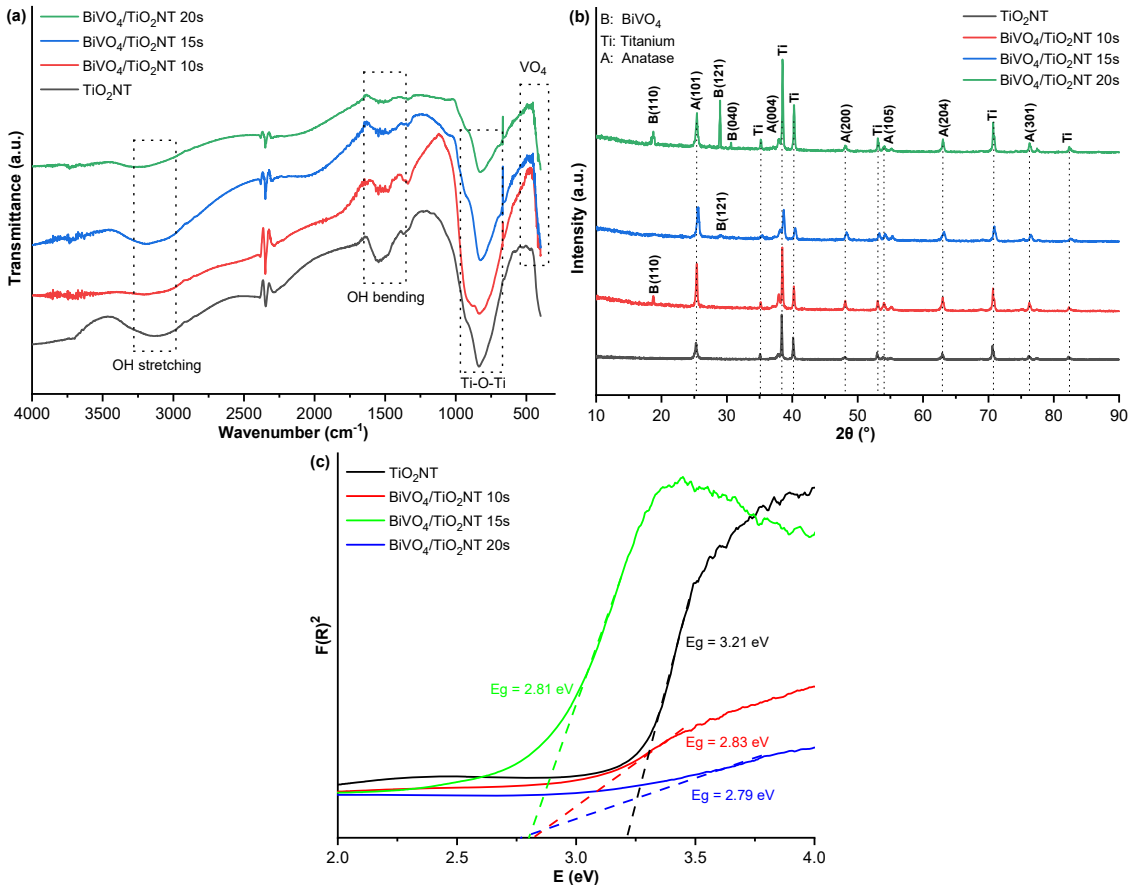

Fig 2. (a) FTIR spectrum; (b) XRD spectra; and (c) the Tauc plot of the Kubelka-Munk function of TiO_2NT and $BiVO_4/TiO_2$NT with SILAR cycle variations

formation of a mixed phase of $BiVO_4/TiO_2$NT heterojunction. The decrease in band gap value indicates that $BiVO_4/TiO_2$NT synthesized by the SILAR method can be active against visible light [21].

The morphology of the synthesized TiO_2NT was then characterized using SEM-EDX. Fig. 3(a) and 3(b) show the morphology of TiO_2 at the surface and cross-section. Based on this figure, it can be observed that TiO_2 formed has nanotube morphology with an average pore diameter of about 56.44 nm and a tube height of 3.11 μm. Several factors affect the morphology of nanotubes, such as the time and anodization potential, the distance between the electrodes, and the composition of the electrolyte [22].

Fig. 3(c) and 3(d) show the SEM results of $BiVO_4/TiO_2$NT 20 cycles (the 20s) surface and cross-section. It can be seen that the yellow $BiVO_4$ has stuck to the surface of the TiO_2NT and does not close the pores so that it can increase the surface area. Fig. 4 shows the EDX spectra of TiO_2NT and $BiVO_4/TiO_2$NT 20s synthesis results. Based on these results, it is known that the synthesized TiO_2NT is composed of Ti and O elements with a ratio of 1:2 atom percentage to form TiO_2. While for the sample $BiVO_4/TiO_2$NT 20s, the percentage atom of Bi:V:Ti:O is 2.1:2.2:26.6:69.1, which shows the amount mass of $BiVO_4$ deposited with 20 cycles is 23.97%.

Fig. 5(a) is the resulting curve for the photoelectrochemical activity of TiO_2NT and $BiVO_4/TiO_2$NT using the Linear Sweep Voltammetry (LSV) method. The results obtained show a comparison of the current density response to the potential between TiO_2NT and $BiVO_4/TiO_2$NT using visible light with a white LED lamp 13 W. The curve shows that $BiVO_4/TiO_2$NT has a higher current density than TiO_2NT. As the number of SILAR cycles increases, the current density response also increases. This indicates

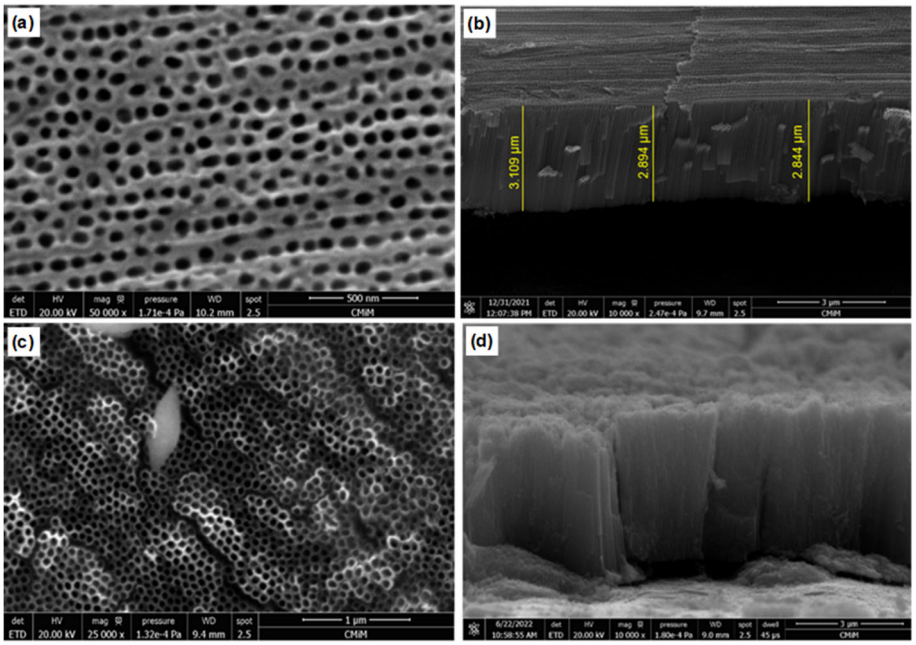

Fig 3. SEM results of (a) TiO_2NT surface 50,000×, (b) TiO_2NT cross-section 10,000×, (c) $BiVO_4/TiO_2$NT surface 25,000× and (d) $BiVO_4/TiO_2$NT cross-section 10,000× with 20 cycles SILAR

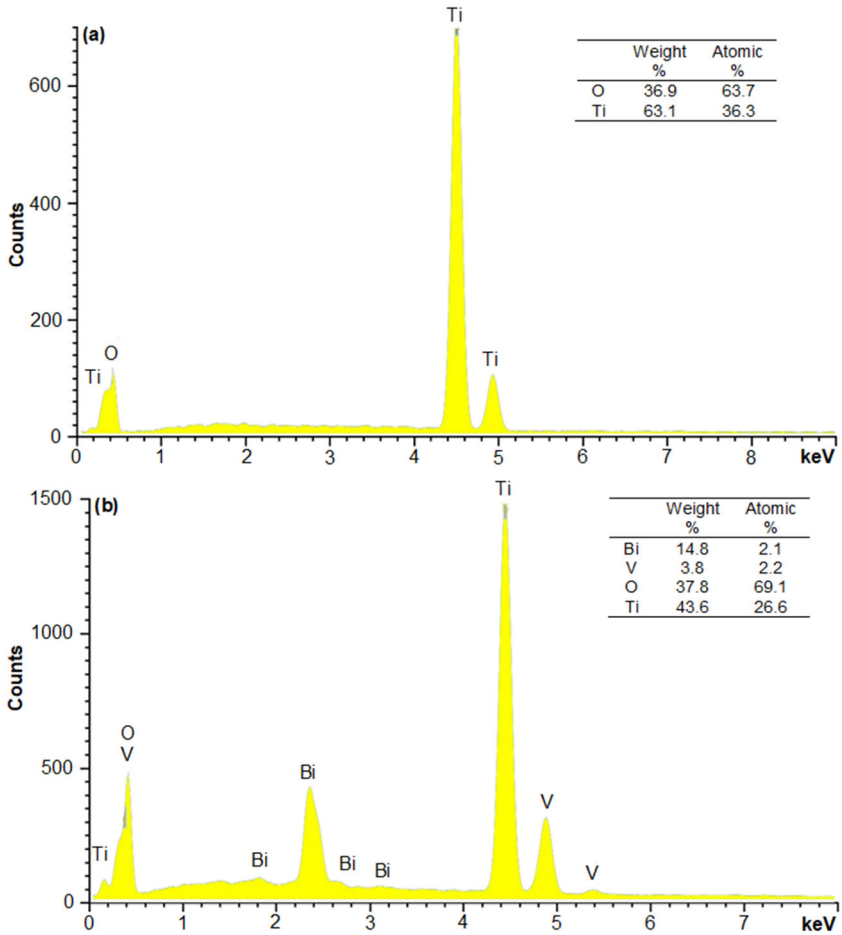

Fig 4. EDX results of (a) TiO_2NT and (b) $BiVO_4/TiO_2$NT with 20 cycles SILAR

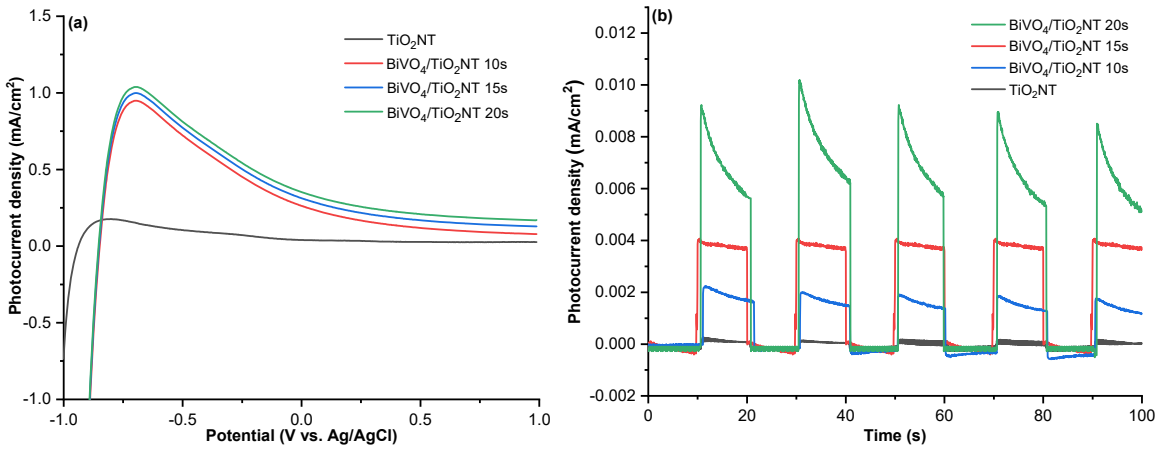

Fig 5. Photocurrent activity results using a potentiostat with 13 W white LED irradiation. Curves of (a) LSV scan rate 25 mV/s and (b) MPA at constant potential 0 V vs. Ag/AgCl

that the addition of $BiVO_4$ on the surface of TiO_2NT can increase the photocatalytic activity of TiO_2NT in the visible light region due to charge separation across the $BiVO_4/TiO_2NT$ interface. Fig. 5(b) is a Multiple Pulse Amperometry (MPA) curves that show the current density response of TiO_2NT and $BiVO_4/TiO_2NT$ on irradiation using visible light. Based on the obtained curve, it shows that $BiVO_4/TiO_2NT$ gives the highest current density response when exposed to visible light. The higher current density response was due to the distribution of $BiVO_4$ formed on the TiO_2NT surface.

In this case, 20 cycles of SILAR showed a higher current density response than 10 and 15 cycles, so the 20 cycles of $BiVO_4/TiO_2NT$ synthesis would be used as a photoanode for the nitrogen reduction reaction to ammonia.

Dark Cathode Characterization of Ti^{3+}/TiO_2NT

In this system, Ti^{3+}/TiO_2NT functions as a dark cathode where the Nitrogen Reduction Reaction (NRR) occurs. The presence of Ti^{3+} species will be the active site as an electron donor for the reduction of nitrogen to ammonia, which causes an easy dissociation of N≡N bonds. With some transformation of surface Ti from Ti^{3+} to Ti^{4+}, electrons will naturally be injected into N_2 [23].

Fig. 6(a) shows the FTIR spectra of TiO_2NT and Ti^{3+}/TiO_2NT at a wavenumber of 4000–400 cm^{-1}. It can be seen that the Ti-O-Ti absorption peak of Ti^{3+}/TiO_2NT at a wave number of 900 cm^{-1} decreases compared to TiO_2NT. This phenomenon is due to reduced Ti-O-Ti bonds at the surface due to the reduction process that can be associated with an increase in the Ti^{3+} population in TiO_2NT. At wave numbers 1700–1400 cm^{-1}, the OH bending functional group indicates that there are water molecules adsorbed on the Ti^{3+}/TiO_2NT surface [24].

Fig. 6(b) shows the UV-Vis spectrum of the Ti^{3+}/TiO_2NT DRS. The band gap value of Ti^{3+}/TiO_2NT can be determined by the Tauc plot of the Kubelka-Munk function, which is 3.13 eV. The band gap value obtained after presenting Ti^{3+} in TiO_2NT, there was a decrease in the band gap from 3.21 to 3.13 eV. The resulting band gap indicates that Ti^{3+}/TiO_2NT is active in UV light.

Fig. 6(c) shows the results of LSV characterization on Ti^{3+}/TiO_2NT irradiated with UV light, visible light, and dark conditions. The LSV test was conducted in the potential range of −1 to 1 V. These results indicate that Ti^{3+}/TiO_2NT irradiated with UV lamps produces a higher current density than in visible light or dark conditions. This is directly proportional to the band gap value of Ti^{3+}/TiO_2NT, which is active against UV light. The high current density indicates that when Ti^{3+}/TiO_2NT is irradiated with a UV lamp, there will be an excitation of electrons from the valence band to the conduction band.

Fig. 6(d) shows the results of the MPA characterization on Ti^{3+}/TiO_2NT within 100 s. The results of this characterization indicate that Ti^{3+}/TiO_2NT

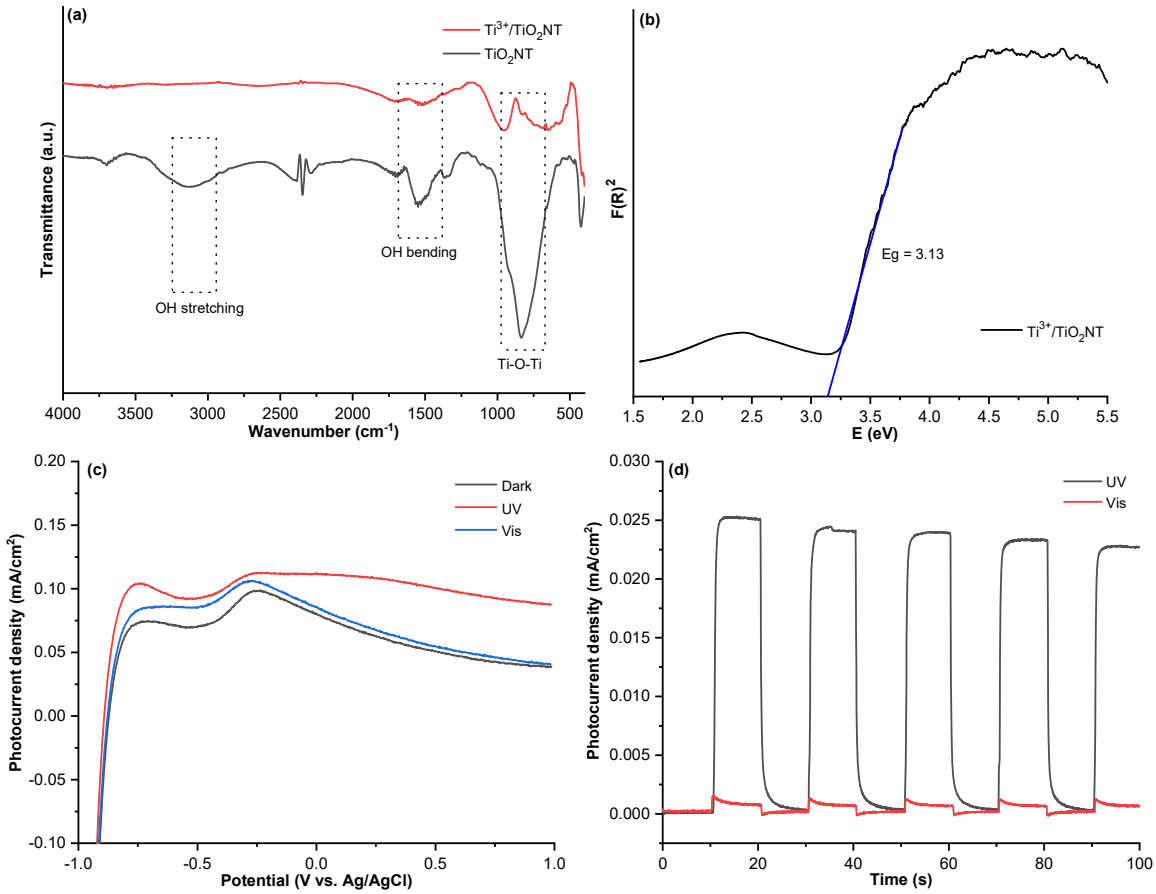

Fig 6. (a) FTIR spectrum, (b) The band gap value using the Tauc plot of the Kubelka-Munk function, (c) Linear Sweep Voltammetry, and (d) Multi Pulse Amperometry of Ti^{3+}/TiO_2NT

responds to UV light. When Ti^{3+}/TiO_2NT is given a UV lamp, there will be an increase in current density, and when the UV lamp is turned off, there will be a significant decrease in current density. This increase in current density indicates that there is an excitation of electrons. At the same time, the decrease in current density indicates that there is a recombination of electrons from the conduction band to the valence band. However, when exposed to visible light, the current density is lower than given UV light. This indicates that the synthesized Ti^{3+}/TiO_2NT has a strong response in the UV region [25].

DSSC Efficiency Characterization

DSSC efficiency test is measured by plotting the current versus potential curve in the range of 0 to 1 Volt. Fig. 7 shows the curve of the change in DSSC current to the given potential when irradiated using visible light from a white LED lamp. From the curve obtained, it can be determined the value of J_{sc}, V_{oc}, P_{max}, P_{in}, fill factor, and efficiency of the DSSC according to the data listed in Table 1. By using a lamp power of 25.5 mW/cm^2 for irradiation, the DSSC cell efficiency is obtained at 1.13%

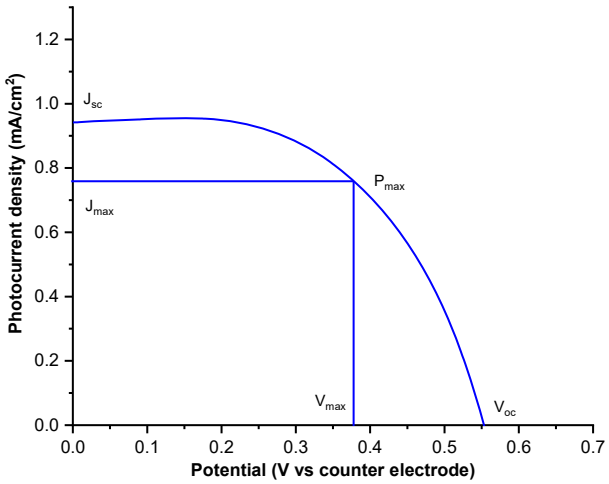

Fig 7. The Current versus Voltage curve of DSSC

Table 1. DSSC efficiency measurement data

J_{max} (mA/cm²)	V_{max} (V)	J_{sc} (mA/cm²)	V_{oc} (V)	P_{max} (mW/cm²)	P_{in} (mW/cm²)	FF	η (%)
0.75941	0.378	0.94188	0.552	0.28706	25.5	0.55212	1.13

with a fill factor value of 0.55212. This DSSC cell will then be used in a DSSC-PEC tandem cell for the reduction of nitrogen into ammonia to increase the electrons that enter the catalysis zone so that more ammonia will be produced.

Tandem System for N_2 Applications

The reaction process for reducing nitrogen to ammonia occurs in the DSSC-PEC tandem system. The nitrogen reduction reaction occurs in the Ti^{3+}/TiO_2NT catalytic zone as the PEC cathode is connected to TiO_2NT/N719 as the DSSC anode. PEC anode, namely $BiVO_4/TiO_2NT$ oxidation reaction, occurs in water to produce electrons (e^-) and protons (H^+). Then H^+ will flow from the anode to the PEC cathode through the Nafion membrane while the electrons (e^-) flow to the Pt/FTO as the DSSC cathode through the external circuit (cable). These electrons are used to reduce I_3^- to I^- ions in DSSC. At the PEC cathode, nitrogen is reduced to ammonia.

At the PEC, dark cathode, there is a nitrogen reduction reaction to ammonia, and at the photoanode, there is an oxidation reaction of water into protons and oxygen according to the following equation:

$$N_2(g) + 6H^+(aq) + 6e^- \rightarrow 2NH_3(g) \quad (3)$$

$$2H_2O(l) \rightarrow 4H^+(aq) + O_2(g) + 4e^- \quad (4)$$

The resulting ammonia then flows into a reservoir containing a 0.01 M HCl solution to produce an ammonium chloride (NH_4Cl) solution.

$$NH_3(g) + HCl(aq) \rightarrow NH_4Cl(aq) \quad (5)$$

Fig. 8 shows experimental data on the amount of ammonia produced at two irradiation conditions (A: dark cathode, B: full irradiation). From the Fig. 8, it can be seen that the ammonia produced increased with increasing reaction time. The amount of ammonia produced in the DSSC+photoanode (A) irradiation region for 2, 4, and 6 h, respectively, was 0.180, 0.253, and 0.393 μmol. The amount of ammonia produced in the DSSC+PEC electrode (B) irradiation region for 2, 4, and 6 h, respectively, was 0.173, 0.240, and 0.320 μmol. These results indicate that the cell system is well-operating under visible light [21]. In addition, the results under full irradiation (Condition B) are lower than the dark cathode (Condition A). It might be caused by when the PEC cathode (Ti^{3+}/TiO_2NT) is irradiated, photon-generated active electrons in its conduction band, and these electrons find antagonistic behavior with electrons from the DSSC part due to the potential bias resulting in the system as a whole [26].

The percentage of energy efficiency in ammonia can be calculated using the Solar to Chemical Conversion (SCC) Eq. (1) [2]. SCC is the ratio between the amount of ammonia produced and the total energy given at a certain time. The free energy for the formation of ammonia from nitrogen gas and water is 399 kJ/mol. Total energy input (Watt) is the amount of light given from the irradiation source to the active area of the DSSC. The light intensity in this study was 3050 lux, which is equivalent to 4,466 W/m² with the irradiated DSSC area of 0.0003 m², so the total input power generated was 0.00134 W. Based on the calculation results

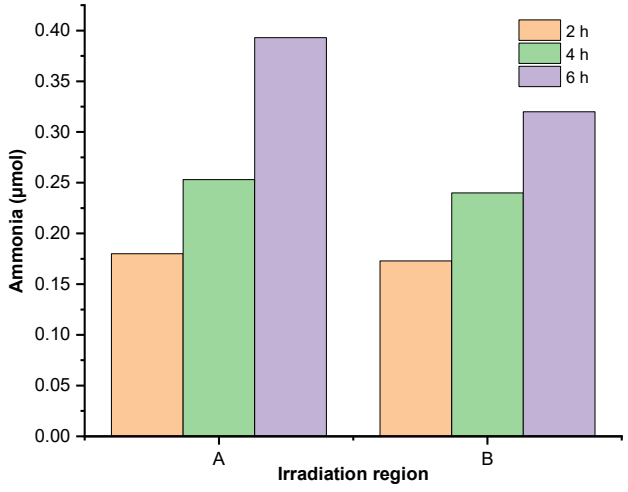

Fig 8. The amount of ammonia produced under various irradiation conditions during the reaction time of 2, 4, and 6 h (A: dark cathode, B: full irradiation)

results, the percentage of SCC for photoanode and dark cathode with a reaction time of 6 h is 0.003%.

■ CONCLUSION

In summary, the authors have successfully synthesized $BiVO_4/TiO_2NT$ heterojunction, which is active in visible light by SILAR method with 3 cycles variations, namely 10, 15, and 20 cycles. Among the others, 20-cycle $BiVO_4/TiO_2NT$ gave the best result as a photoanode, characterized by the smallest band gap energy and the highest photocurrent density for water oxidation (0.352 mA/cm^2). In addition, for the NRR, the $BiVO_4/TiO_2NT$ photoanode was used along with Ti^{3+}/TiO_2NT cathode in the PEC system coupled with a DSSC based on TiO_2NT/N719 with an efficiency of 1.13% as an energy booster in the reaction. The DSSC-PEC tandem system under "A" condition (Dark cathode, irradiation on DSSC and photoanode) resulted in SCC efficiency of 0.003% and ammonia production of 0.022 $mol.h^{-1}.cm^{-2}$. Although still lacking, the result shows that the tandem DSSC-PEC system was able to reduce nitrogen (N_2) to ammonia (NH_3) with only visible light irradiation. There are many aspects that can be optimized for future development. First, the activity of the photoanode site could be enhanced more by further optimizing the amount of $BiVO_4$ deposited and directing the crystal growth on the active facets. Second, further optimization on DSSC efficiency and Ti^{3+} population as the active size at the cathode is predicted to be able to improve the performance of the whole system. Third, finding the best environment, such as electrolyte, temperature, also system design, especially at the cathode site, to enhance the selectivity of the system to NRR is still believed to be a major factor that should be addressed in future work. Thus, this work is expected to stimulate the development of the catalyst and system design for a better NRR visible active–photo(electro)catalytic system in the future.

■ ACKNOWLEDGMENTS

The authors gratefully acknowledge the support from DGHE, Directorate General of Higher Education, for funding the research (PDUPT research contract No. NKB-174/UN2.RST/HKP.05.00/2021).

■ REFERENCES

[1] Chen, Q., Fan, G., Fu, H., Li, Z., and Zou, Z., 2018, Tandem photoelectrochemical cells for solar water splitting, *Adv. Phys.: X*, 3 (1), 1487267.

[2] Hirakawa, H., Hashimoto, M., Shiraishi, Y., and Hirai, T., 2017, Photocatalytic conversion of nitrogen to ammonia with water on surface oxygen vacancies of titanium dioxide, *J. Am. Chem. Soc.*, 139 (31), 10929–10936.

[3] Licht, S., Cui, B., Wang, B., Li, F.F., Lau, J., and Liu, S., 2014, Ammonia synthesis by N_2 and steam electrolysis in molten hydroxide suspensions of nanoscale Fe_2O_3, *Science*, 345 (6197), 637–640.

[4] Li, C., Wang, T., and Gong, J., 2020, Alternative strategies toward sustainable ammonia synthesis, *Trans. Tianjin Univ.*, 26 (2), 67–91.

[5] Liu D., Wang, J., Bian, S., Liu, Q., Gao, Y., Wang, X., Chu, P.K., and Yu, X.F., 2020, Photoelectrochemical synthesis of ammonia with black phosphorus, *Adv. Funct. Mater.*, 30 (24), 2002731.

[6] Liu, Q.Y., Wang, H.D., Tang, R., Cheng, Q., and Yuan, Y.J., 2021, Rutile TiO_2 nanoparticles with oxygen vacancy for photocatalytic nitrogen fixation, *ACS Appl. Nano Mater.*, 4 (9), 8674–8679.

[7] Dong, H., Zeng, G., Tang, L., Fan, C., Zhang, C., He, X., and He, Y., 2015, An overview on limitations of TiO_2-based particles for photocatalytic degradation of organic pollutants and the corresponding countermeasures, *Water Res.*, 79, 128–146.

[8] Zhang, X., Yang, H., Zhang, B., Shen, Y., and Wang, M., 2016, BiOI-TiO_2 nanocomposites for photoelectrochemical water splitting, *Adv. Mater. Interfaces*, 3 (1), 1500273.

[9] Syauqi, M.I., Prasetia, P., and Gunlazuardi, J., 2023, The influence of sodium alginate in water-based electrolyte on the morphology of TiO_2 nanotube prepared by anodization method, *Mater. Chem. Phys.*, 296, 127234.

[10] Yunita, Y., Syauqi, M.I., and Gunlazuardi, J., 2022, Comparative study of bismuth ferrite deposition method on TiO_2 nanotube and performance of hydrogen evolution in a photoelectrochemical dye-

sensitized solar cell tandem system, *Makara J. Sci.*, 26 (3), 190–199.

[11] Zhu, X., Zhang, F., Wang, M., Gao, X., Luo, Y., Xue, J., Zhang, Y., Ding, J., Sun, S., Bao, J., and Gao, C., 2016, A shuriken-shaped *m*-$BiVO_4$/{001}–TiO_2 heterojunction: Synthesis, structure and enhanced visible light photocatalytic activity, *Appl. Catal., A*, 521, 42–49.

[12] Surahman, H., 2017, Pengembangan Sel Fotoelektrokimia Menggunakan Elektroda TiO_2 Nanotube Arrays Tersensitisasi CdS Nanopartikel untuk Produksi Hidrogen, *Dissertation*, Universitas Indonesia.

[13] Samsudin, M.F.R., Sufian, S., Mohamed, N.M., Bashiri, R., Wolfe, F., and Ramli, R.M., 2018, Enhancement of hydrogen production over screen-printed TiO_2/$BiVO_4$ thin film in the photoelectrochemical cells, *Mater. Lett.*, 211, 13–16.

[14] Song, J., Zheng, M., Yuan, X., Li, Q., Wang, F., Ma, L., You, Y., Liu, S., Liu, P., Jiang, D., Ma, L., and Shen, W., 2017, Electrochemically induced Ti^{3+} self-doping of TiO_2 nanotube arrays for improved photoelectrochemical water splitting, *J. Mater. Sci.*, 52 (12), 6976–6986.

[15] Shi, L., Xu, C., Sun, X., Zhang, H., Liu, Z., Qu, X., and Du, F., 2018, Facile fabrication of hierarchical $BiVO_4$/TiO_2 heterostructures for enhanced photocatalytic activities under visible-light irradiation, *J. Mater. Sci.*, 53 (16), 11329–11342.

[16] Ramakrishnan, V.M., Pitchaiya, S., Muthukumarasamy, N., Kvamme, K., Rajesh, G., Agilan, S., Pugazhendhi, A., and Velauthapillai, D., 2020, Performance of TiO_2 nanoparticles synthesized by microwave and solvothermal methods as photoanode in dye-sensitized solar cells (DSSC), *Int. J. Hydrogen Energy*, 45 (51), 27036–27046.

[17] Orimolade, B.O., and Arotiba, O.A., 2019, An exfoliated graphite-bismuth vanadate composite photoanode for the photoelectrochemical degradation of acid orange 7 dye, *Electrocatalysis*, 10 (4), 429–435.

[18] Raidou, A., Benmalek, F., Sall, T., Aggour, M., Qachaou, A., Laanab, L., and Fahoume, M., 2014, Characterization of ZnO thin films grown by SILAR method, *Open Access Libr. J.*, 1 (3), 1–9.

[19] Dette, C., Perez-Osorio, M.A., Kley, C.S., Punke, P., Patrick, C.E., Jacobson, P., Giustino, F., Jung, S.J., and Kern, K., 2014, TiO_2 anatase with a bandgap in the visible region, *Nano Lett.*, 14 (11), 6533–6538.

[20] Wu, M., Jing, Q., Feng, X., and Chen, L., 2018, $BiVO_4$ microstructures with various morphologies: Synthesis and characterization, *Appl. Surf. Sci.*, 427, 525–532.

[21] Drisya, K.T., Solís-López, M., Ríos-Ramírez, J.J., Durán-Álvarez, J.C., Rousseau, A., Velumani, S., Asomoza, R., Kassiba, A., Jantrania, A., and Castaneda, H., 2020, Electronic and optical competence of TiO_2/$BiVO_4$ nanocomposites in the photocatalytic processes, *Sci. Rep.*, 10 (1), 13507.

[22] Macak, J.M., Hildebrand, H., Marten-Jahns, U., and Schmuki, P., 2008, Mechanistic aspects and growth of large diameter self-organized TiO_2 nanotubes, *J. Electroanal. Chem.*, 621 (2), 254–266.

[23] Chen, X., Li, N., Kong, Z., Ong, W.J., and Zhao, X., 2018, Photocatalytic fixation of nitrogen to ammonia: State-of-the-art advancements and future prospects, *Mater. Horiz.*, 5 (1), 9–27.

[24] Budiman, H., Wibowo, R., Zuas, O., and Gunlazuardi, J., 2021, Effect of annealing temperature on the characteristic of reduced highly ordered TiO_2nanotube arrays and their CO gas-sensing performance, *Process. Appl. Ceram.*, 15 (4), 417–427.

[25] Zhu, Y., Shah, M.W., and Wang, C., 2016, Insight into the role of Ti^{3+} in photocatalytic performance of shuriken-shaped $BiVO_4$/TiO_{2-x} heterojunction, *Appl. Catal., B*, 203, 526–532.

[26] An'Nur, F.K., Wihelmina, B.V., Gunlazuardi, J., and Wibowo, R., 2020, Tandem system of dyes sensitized solar cell–photo electro chemical (DSSC-PEC) employing TiO_2 nanotube/BiOBr as dark cathode for nitrogen fixation, *AIP Conf. Proc.*, 2243, 020002.